



This is an open access article distributed under the terms of the Creative Commons Attribution 4.0 International License (CC BY 4.0), which permits use, distribution, and reproduction in any medium, provided the original publication is properly cited. No use, distribution or reproduction is permitted which does not comply with these terms.

# EXTERNAL MONITORING SYSTEM FOR BATTERY CONDITION AND STATE OF HEALTH OF LITHIUM-ION BATTERIES

Milan Havelka<sup>1</sup>, Matúš Nečas<sup>2</sup>, Dušan Maga<sup>3</sup>, Juraj Dudák<sup>1,2,\*</sup>


<sup>1</sup>Slovak University of Technology in Bratislava, Faculty of Materials Science and Technology in Trnava, Institute of Applied Informatics, Automation and Mechatronics, Trnava, Slovak Republic

<sup>2</sup>University of Žilina, Research Centre, Žilina, Slovak Republic

<sup>3</sup>Czech Technical University in Prague, Faculty of Electrical Engineering CTU in Prague, Prague, Czech Republic

\*E-mail of the corresponding author: juraj.dudak@stuba.sk

Milan Havelka  0009-0005-1706-155X,  
Dusan Maga  0000-0001-8176-2151,

Matus Necas  0009-0002-5145-2835,  
Juraj Dudak  0000-0002-5570-5150

## Resume

Lithium-ion batteries power light electric vehicles such as electric bicycles, but end users typically lack reliable information about true battery health and instead rely on misleading indicators of remaining charge. In this paper is introduced a novel external plug-and-play diagnostic module that connects between the standard charger and a battery of a light electric vehicle. The system uses a precise discrete-time energy integration method during standard charging. It captures dynamic current fluctuations and estimates battery health from the partial charging data. Experimental validation on multiple battery packs demonstrates that the proposed algorithm reliably distinguishes between healthy and degraded batteries. This non-invasive system adds diagnostics to conventional charging, enabling users to assess actual capacity without full discharge cycles.

## Article info

Received 2 March 2026

Accepted 28 March 2026

Online 22 April 2026

## Keywords:

capacity fade  
condition monitoring  
energy integration  
light electric vehicles  
lithium-ion batteries  
state of health

Available online: <https://doi.org/10.26552/com.C.2026.028>

ISSN 1335-4205 (print version)

ISSN 2585-7878 (online version)

## 1 Introduction

The development of modern transportation systems, along with the need to reduce greenhouse gas emissions in urban areas, has driven the widespread adoption of electrically powered vehicles in daily life. The shift to electric transport has become central to sustainable transportation, with its success depending on the availability, performance, and lifespan of energy storage systems, especially lithium-ion (Li-Ion) batteries. Efforts to maximize battery lifespan hold immense economic value and critical ecological significance, as the production and recycling of battery cells represent a considerable environmental burden and require advanced lifecycle management. From the standpoint of technological complexity and infrastructure requirements, electric mobility can be divided into three main categories: mass and freight transport (electric buses and trucks), standard passenger transport (electric vehicles), and simple personal micromobility, commonly called light electric vehicles, such as e-bicycles and e-scooters [1]. While passenger EVs and public transport systems use

sophisticated Battery Management Systems (BMS) with active thermal management and precise State of Health (SOH) diagnostics, the LEV category significantly lags in this area. In simple personal micromobility, BMS architectures are often limited to basic overcharge and overdischarge protection. The LEV users typically lack access to reliable information about the actual health and remaining capacity of their batteries. Instead, they must rely on a basic and often misleading State of Charge (SOC) indicator, usually based only on instantaneous terminal voltage [2]. This significant disparity in battery management underscores the urgent need for improved diagnostics in the LEV category. The lack of accurate SOH information leads to improper charging habits, which accelerate battery degradation and reduce overall lifespan. Therefore, there is a growing demand for diagnostic devices that are accessible, external, and flexible.

Accumulators, such as rechargeable batteries (also called secondary batteries), are a key technology in energy storage, enabling repeated charging and discharging through reversible electrochemical

reactions. While this work primarily focuses on Li-Ion batteries, understanding their market position and scientific context requires a brief overview of the main competing technologies. Currently, Li-Ion batteries are among the most widely used energy storage systems in portable electronics, electromobility, and industrial applications. Their widespread adoption is mainly due to their high energy density, low weight, and relatively long lifespan compared to traditional accumulators. These characteristics have made Li-Ion batteries the standard choice for devices that require low weight, compact design, and high energy efficiency, including smartphones, laptops, electric vehicles, drones, and renewable energy systems. The energy density of Li-Ion batteries is approximately 150 to 250 Wh/kg, a significant advantage over older technologies [3]. In addition, they have relatively low self-discharge rates, making them suitable for the long-term storage.

Although the charging and discharging process of a Li-Ion battery is theoretically reversible, practical applications involve gradual losses caused by side chemical reactions, the formation of passivation layers, and mechanical degradation of electrodes. These phenomena result in capacity fade, increased internal resistance, and a gradual reduction in the battery's lifespan. Li-Ion batteries are produced in various mechanical designs. The most commonly used are cylindrical cells with a metal casing, prismatic cells with a rigid shell, and pouch cells with a flexible enclosure. Each type has specific characteristics regarding mechanical durability, cooling options, and integration into battery systems [4]. The selection of an appropriate cell type depends on the specific application, required power output, available space, and safety requirements.

The life cycle of Li-Ion batteries includes all phases from manufacturing, through operation, to end-of-life disposal. A proper understanding of the individual life cycle phases is essential for designing systems capable of effectively monitoring, protecting, and extending battery longevity. In battery monitoring systems, it is particularly important to track operational conditions, as these have a direct impact on battery degradation [5].

The operational phase is the longest and most significant part of the life cycle of a Li-Ion battery. During this phase, the battery is repeatedly charged and discharged depending on the application. Each charge-discharge cycle contributes to the gradual degradation of the cell, which appears as a decrease in capacity, an increase in internal resistance, and a deterioration of performance parameters [6]. The rate of degradation is significantly influenced by operating conditions, particularly temperature, charging and discharging current magnitudes, the operating voltage range, and the Depth of Discharge (DoD). Adverse conditions can substantially shorten

the battery's lifespan and increase the risk of failure.

The aging of a Li-Ion battery is a complex process involving a combination of chemical, electrochemical, and mechanical phenomena within the cell. A distinction is made between calendar aging, which occurs even when the battery is not cycled, and cyclic aging, which is caused by repeated charging and discharging. The main manifestations of aging include the loss of active lithium inventory, degradation of electrode materials, an increase in internal resistance, and a reduction in the battery's ability to deliver high currents. These processes are largely irreversible [7] and gradually limit the battery's usability in its primary application.

### 1.1 Safety aspects during the life cycle

The safety of Li-Ion batteries is critical throughout their entire life cycle. Improper operation, mechanical damage, or exceeding permissible temperature and voltage limits can lead to hazardous events such as overheating, cell swelling, or, in extreme cases, thermal runaway [8]. For these reasons, modern applications increasingly use protection and monitoring systems that continuously track key battery parameters and, if necessary, alert the user or restrict the operation of the system. Such continuous monitoring throughout the life cycle significantly improves the safety, reliability, and lifespan of battery systems.

The end of life for a Li-Ion battery is generally considered to be the point at which its usable capacity drops below a specified threshold, most commonly around 70 % to 80 % of its initial nominal capacity. In this state, the battery may no longer meet the requirements of its original application; however, it can still be repurposed for less demanding systems [9]. The conclusion of primary use is followed by a secondary use phase (second life) or recycling, aimed at minimizing the environmental footprint while recovering valuable materials. Efficient life cycle management of Li-Ion batteries is therefore crucial not only from a technical and safety standpoint but also from an ecological perspective.

The SOC represents the ratio of the currently available battery capacity to its nominal capacity, usually expressed as a percentage. It is one of the most important parameters for both the user and the management system, as it indicates the remaining energy in the battery. However, the SOC cannot be measured directly and must be estimated using various computational methods. One of the most common methods is current integration, known as Coulomb counting, which tracks the amount of electrical charge supplied to or drawn from the battery during operation [10]. The main drawback of this method is the gradual accumulation of errors due to current measurement inaccuracies

and the absence of a precise initial SOC value. An alternative approach uses voltage-based methods, where the instantaneous voltage is compared to the cell's characteristic open-circuit voltage (OCV) curve. While simple to implement, this method has limited accuracy, especially under load or during dynamic current fluctuations [11].

In addition to the SOC, another key parameter is the SOH, which quantifies the degree of battery degradation compared to a new cell. The SOH is typically defined as the percentage ratio of the current maximum available capacity to the original nominal capacity. The decline in SOH is a natural result of battery aging and long-term operation. The primary degradation mechanisms include chemical degradation of electrodes, loss of active lithium, and an increase in the internal resistance of the cell. Monitoring the SOH is essential for estimating the Remaining Useful Life (RUL) of the battery, enhancing operational safety, and planning for battery replacement or repurposing in less demanding applications. The SOH is estimated based on long-term observation of charging and discharging cycles, capacity measurements, or analysis of changes in the battery's internal resistance [12].

The primary motivation for this study stems from the need to determine the actual remaining capacity of commonly used lithium-ion batteries, since this key indicator of battery health is typically not available to end users. Therefore, the objective of this research was to design and implement an SOH estimation algorithm embedded within a dedicated health-monitoring device for standard light LEVs, such as e-bicycles and e-scooters. The proposed system is designed to operate continuously during standard charging cycles. By analyzing dynamic charging parameters and specific battery characteristics, the device can accurately estimate the actual battery capacity.

The main goals of this research were:

- Design and implementation of a flexible, external data acquisition system: Development of a non-invasive condition monitoring device capable of logging main operational parameters (voltage, current, temperature) for LEV lithium-ion batteries without interfering with the internal BMS.
- Comprehensive experimental evaluation of battery cycling: Execution of repeated charging and discharging cycles on standard micromobility battery packs (e.g., e-bicycles, e-scooters) to capture real-world degradation patterns and capacity fade over time.
- Development and validation of a practical SOH estimation algorithm: Proposal of an algorithm to accurately estimate the SOH and evaluate the remaining useful life of the batteries, validated against the collected experimental dataset.

## 2 Materials and methods

Determining the SOH in practical applications is significantly more challenging than estimating the SOC, as it is a slowly varying parameter that cannot be directly measured by conventional physical sensors. The accuracy of SOH estimation depends heavily on the chosen mathematical model and the quality of the input data. Currently, the Li-Ion battery diagnostics primarily use methods based on tracking capacity degradation and internal resistance growth. The most straightforward approach is the direct capacity measurement method (Ah-method) [13], which compares the actual charge transferred during a full cycle with the nominal capacity of a new battery. Although highly accurate, this method requires a complete discharge and charge cycle under controlled conditions, which is often unfeasible in real-world operation. An alternative is monitoring the increase in Direct Current Internal Resistance (DCIR) [14], calculated based on the voltage response to a step change in current. The rise in internal resistance is a direct consequence of electrolyte aging and the formation of passivation layers on the electrodes. For applications requiring real-time SOH estimation, advanced model-based approaches, running directly within the BMS control unit, are employed [15]. These algorithms use Equivalent Circuit Models (ECM) that simulate the dynamic behavior of the battery with a network of resistors and capacitors. In state-of-the-art systems, data-driven methods are gaining traction; these leverage neural networks to identify nonlinear correlations between operational data and battery degradation, eliminating the need for an in-depth understanding of the internal electrochemical processes of the cell [16].

### 2.1 Basic quantities and principles of Li-Ion battery monitoring

Monitoring operational variables is a fundamental prerequisite for the safe and efficient operation of Li-Ion batteries. The most critical monitored parameters include electrical quantities - primarily voltage and current - as well as battery temperature. These data points provide vital information regarding the instantaneous state of the battery, its load, and potential operational risks. External monitoring devices are a distinct category of solutions connected to the battery without intruding into its internal architecture. These devices enable the measurement of voltage, current, and temperature during battery operation and often feature a visual user interface. The primary advantage of external solutions is their versatility and compatibility across various battery types.

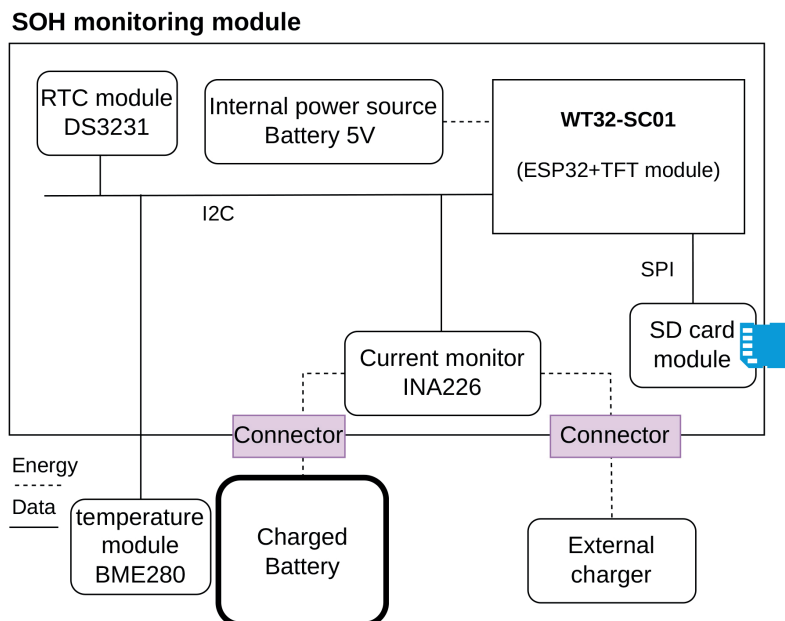


Figure 1 Principal block connection diagram

Table 1 List of used batteries

Label	Battery	Volage	Capacity
B1..B4	CNHL 4S	16.8 V	22.2 Wh
B5	Turnigy 2S	7.4 V	13.32 Wh

**System architecture and hardware setup**

The proposed external condition monitoring system was designed as an independent, non-invasive diagnostic unit. The core of the hardware architecture is the ESP32 microcontroller, selected for its robust processing capabilities and the extensive peripheral interface support. The ESP32 microcontroller is a part of the WT32-SC01 development board with a 3.5-inch color touch screen with a resolution of 320x480 pixels. To ensure the high-precision data acquisition during the battery charging process, a dedicated ADS1015 analog-to-digital converter (ADC) was used, rather than the microcontroller’s internal ADC.

The electrical parameters are monitored using an INA226 power monitor integrated circuit (IC), which is connected via the I<sup>2</sup>C bus. This sensor continuously measures the charging current and battery voltage with high accuracy. The temperature of the battery pack and the ambient environment is monitored using the BME280 sensor. To ensure accurate time integration for capacity calculations and precise temporal data logging, a DS3231 Real-Time Clock (RTC) module is included in the system.

During the charging cycle, all monitored parameters - voltage, current, temperature, and elapsed time - are sampled continuously and logged to an external microSD card via the SPI interface. This comprehensive dataset forms the primary input for the subsequent SOH estimation algorithm. The

system also includes a graphical touch interface for the real-time visualisation of the charging status, current SOC, and the estimated SOH (for example, tested on a 4S Li-Po configuration).

**Battery specifications and charging protocol**

The following batteries (Table 1) were used for this experiment.

A SkyRC<sup>1</sup> charger was used for charging. It is used to manage LiPo/LiHV/LiFe/LiIon (1-6S), NiMH/NiCd (1-15S) and Pb (2-20 V) batteries with capacities ranging from 100 to 50,000 mAh. The device provides a continuously adjustable charging current from 0.1 to 10 A and a balancing current of max. 300 mA per cell. The charging power with DC power supply reaches 2 x 100 W, while with an AC mains power supply it offers a total of 100 W with the possibility of asymmetrical distribution between the two outputs. Secondary, the device can be used as a laboratory power supply with a fixed voltage of 13.8 V and a power of up to 100 W [17].

For lithium (LiPo, LiHV, LiIon, LiFe) and lead (Pb) cells, the charger uses a CC/CV (Constant Current / Constant Voltage) algorithm. In the first phase, it applies a constant current (CC) until the maximum threshold voltage is reached. It then switches to the constant voltage (CV) phase, during which the charging current asymptotically approaches zero. Voltage balancing: For

<sup>1</sup> [https://www.skyrc.com/D100\\_v2\\_Charger](https://www.skyrc.com/D100_v2_Charger)

lithium kits (from 2S to 6S), the voltage of individual cells is monitored and balanced via JST-XH ports using a passive balancing method with a limit current of 300 mA.

### Data acquisition and SOH estimation algorithm

To accurately estimate the initial State of Charge ( $SOC_{start}$ ), the proposed system requires the battery to be in a resting state before charging. The external device measures the Open-Circuit Voltage (OCV), allowing the microcontroller to derive  $SOC_{start}$  using a known dependency model [18]. This resting state measurement mitigates estimation errors caused by voltage drops across the internal resistance.

### Energy Integration

Once the charging process is initiated, the system samples the instantaneous terminal voltage  $U_k$  and the charging current  $I_k$  at a frequency of 1 Hz. The total delivered electrical energy,  $E_{delivered}$  (in Wh), is calculated using discrete time integration:

$$E_{delivered} = \sum_{k=1}^N U_k I_k \Delta t \quad (1)$$

where  $N$  is the total number of samples during the charge cycle, and  $\Delta t$  represents the sampling period converted to hours [19].

**Capacity extrapolation and SOH calculation** - The measurement concludes when the charging current drops below a predefined cutoff threshold (e.g., 0.3 A during the Constant Voltage phase), indicating that the battery has reached approximately 100 % SOC. The change in the State of Charge ( $\Delta SOC$ ), supplied during the measured cycle, is defined as:

$$\Delta SOC = 1 - \frac{SOC_{start}}{100}. \quad (2)$$

Based on the partially delivered energy and the corresponding  $\Delta SOC$ , the system extrapolates the estimated maximum actual capacity of the battery,  $E_{estimated}$ :

$$E_{estimated} = \frac{E_{delivered} \cdot \eta}{\Delta SOC}, \quad (3)$$

where  $\eta$  represents the Coulombic and energy efficiency factor to account for thermal losses during charging. Finally, the State of Health is quantified by comparing the extrapolated real capacity to the nominal capacity ( $E_{nominal}$ ) provided by the user configurations:

$$SOH = \left( \frac{E_{estimated}}{E_{nominal}} \right) \times 100. \quad (4)$$

To account for initial manufacturing variances, where the new cells might slightly exceed their nominal specifications, the algorithm caps the maximum SOH output at 105 %.

When measuring the total SOC, it is important to identify when the battery has reached its maximum charge. The battery charging process was terminated when the following conditions were met:  $OCV \geq 4.2$  V and charging current  $I \leq 0.3$  A. The actual battery capacity is then calculated (according to Equation (1)) and the battery health is evaluated according to Equation (4).

## 3 Results and discussion

As was stated at the beginning of this paper, the aim of this project was to design and implement of a flexible, external data acquisition system with a practical SOH estimation algorithm. The basic architecture is shown in Figure 1. The design uses an ESP32 microcontroller with a built-in display, which is used as an information module during battery charging (Figure 2).

To verify the functionality of the proposed device, 5 batteries were used (Table 1). The charger used had accurate power output measurements, which were used as reference values for the device.

The Final SOC values in Table 2 are calculated according to Equation (4). In the calculation, is considered a capacity of 22.2 Wh for batteries B1 to B4 and a capacity of 13.32 Wh for battery B5.

Graphs in Figure 3 present comprehensive charging profiles - specifically, charging voltage and current as functions of time - for all five batteries

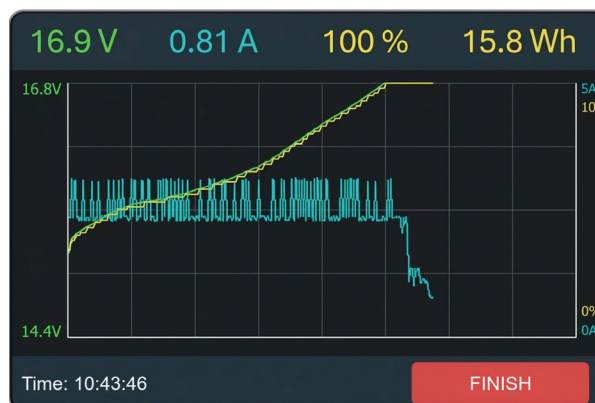


**Figure 2** Monitoring of battery charging process

**Table 2** Charging results

Battery	Start level	Delivered E	Final SOH
B1	0 %	18.95 Wh	89.8 %
B2	0 %	20.65 Wh	93.0 %
B3	15 %	18.8 Wh	99.6 %
B4	5 %	19.9 Wh	94.4 %
B5	33 %	4.8 Wh	53.8 %

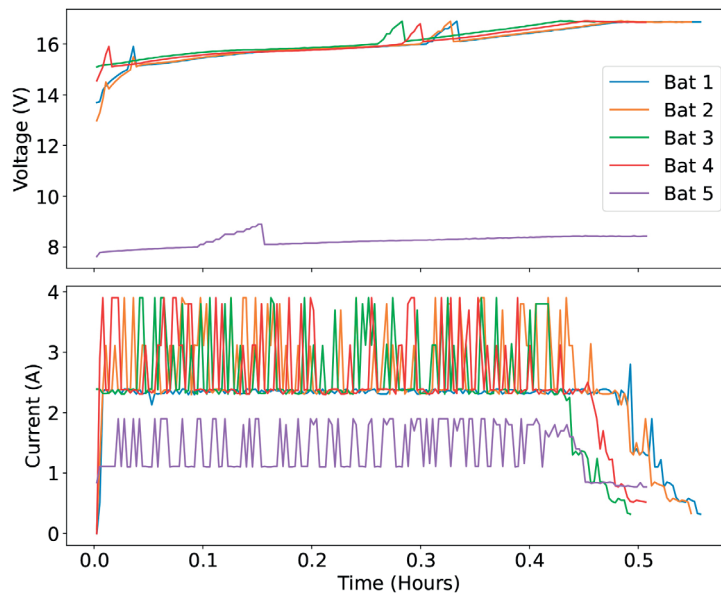


**Figure 3** The charging process monitored by our device

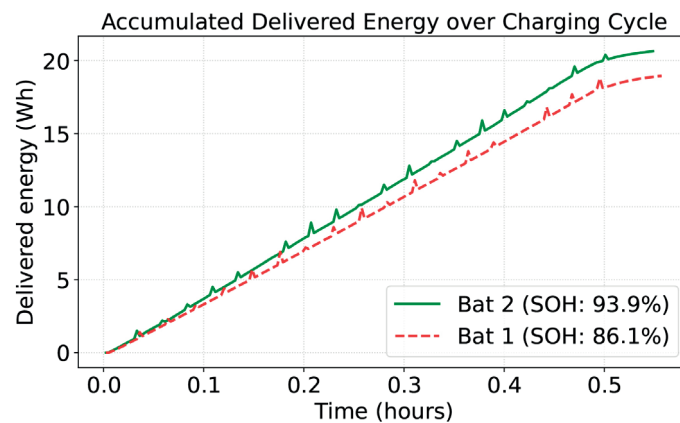


**Figure 4** Accumulated delivered energy over time during a charging cycle for a healthy (Bat 2) and a degraded (Bat 1) battery, both starting from 0 % SOC

tested. The data confirm that the external monitoring system reliably records the standard constant current and constant voltage (CC-CV) charging protocol across different operating conditions and battery configurations. The voltage graph (top section) clearly distinguishes the architectures of the individual batteries. Batteries 1 to 4 have a 4S configuration, gradually approaching their maximum cut-off voltage

of approximately 16.8 V during charging. In contrast, battery 5 has a 2S configuration and operates at a significantly lower voltage level, with a maximum limit of around 8.4 V.

The graph in Figure 3 (bottom) clearly highlights the transition between the CC and CV phases. During the initial CC phase, the charging current remains relatively high and stable until it reaches the battery’s

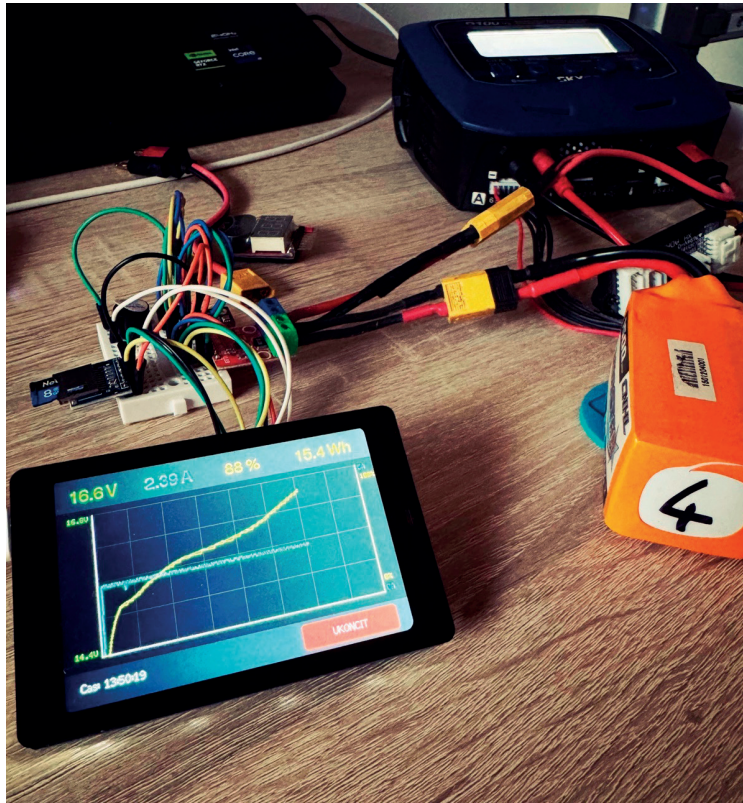


**Figure 5** Prototype of the external condition monitoring module, functioning as an intermediary diagnostic interface between a standard charger and the Li-Ion battery

cut-off voltage. The charging process then transitions to the CV phase, where the current decreases exponentially until it falls below a predefined limit (e.g., 0.3 A), at which point charging is terminated.

In addition, different lengths of the charging cycles directly reflect the different initial charge states (e.g., battery 3 started the measurement at 15 % SOC, while battery 2 started at 0 % SOC), as well as the different levels of degradation and capacity loss of the individual cells.

Graph in Figure 4 shows the accumulation of delivered electrical energy during a charging cycle for two different battery packs, both starting from a completely discharged state (0 % SOC). As charging progresses, continuous discrete integration of electrical power reveals a significant difference in the total absorbed energy.

Although the charging cycle for both batteries ends when the current drops below the cutoff threshold - indicating 100 % relative SOC-the absolute energy capacity differs substantially. The healthy battery (Bat 2) accumulates a total of 20.65 Wh, while the slightly degraded battery (Bat 1) absorbs only 18.95 Wh before reaching the maximum voltage limit.

This 1.7 Wh difference clearly demonstrates capacity fade caused by battery aging. More importantly, it highlights the critical limitation of

relying solely on the standard SOC indicator. While the BMS reports a *fully charged* state for both batteries, the degraded cell holds significantly less actual usable energy for the electric vehicle. This finding strongly supports the need for the proposed external monitoring device, which addresses this information gap by calculating the true SOH based on actual energy integration.

Furthermore, the experimental data revealed discrete fluctuations and step changes in the charging current, particularly during the Constant Current (CC) phase. These variations are primarily due to the discrete regulation mechanisms of commercial switch-mode power supply (SMPS) chargers typically used for micromobility, which do not provide an ideal, continuous current output. The presence of these real-world anomalies strongly underscores the necessity and robustness of the proposed high-frequency (1 Hz) discrete-time energy integration method. The used method of continuous sampling approach effectively captures dynamic fluctuations, ensuring high accuracy in calculating the total delivered energy and the subsequent SOH.

To demonstrate the practical applicability of the proposed solution, the physical monitoring module was constructed as a standalone, plug-and-play add-on device. Figure 5 shows the final hardware prototype in operation.

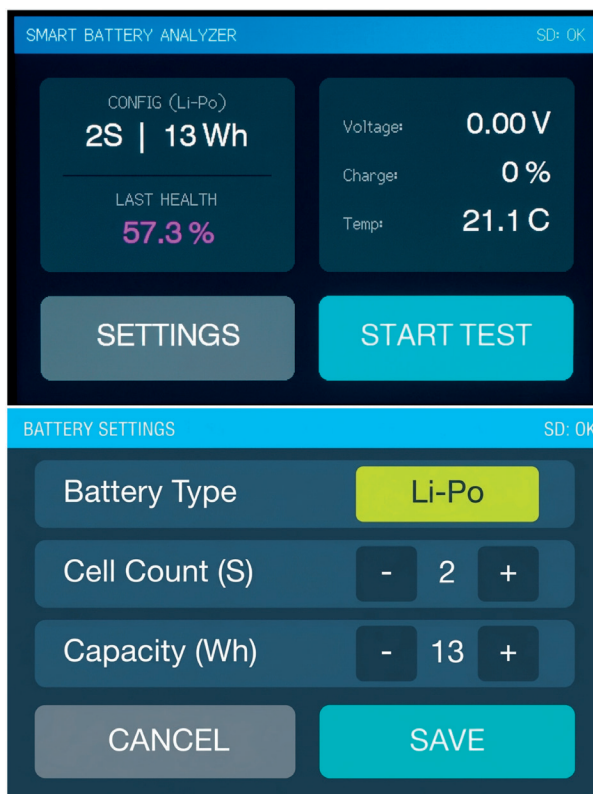


**Figure 6** Graphical user interface of proposed solution - setting of parameters

Figure 6 shows the app's settings: battery type selection (Li-Po or Li-Ion), number of cells, and total battery capacity specified by the manufacturer.

The system is designed to connect in series directly between a conventional charger and the lithium-ion battery pack. A significant economic and practical advantage of this topology is its versatility. It operates on the premise that a basic, standard charger, serving solely as a power supply, is sufficient for the charging process, as all intelligent monitoring, data acquisition, and diagnostic algorithms are fully handled by the proposed external module.

During the charging cycle, the integrated graphical user interface (GUI) provides the end user with continuous, real-time feedback. It displays the instantaneous charging parameters, the dynamically calculated SOC, and the total accumulated energy delivered to the battery. By making these previously hidden metrics visible, the module transforms any standard charging setup into an advanced diagnostic station, giving users a clear, real-time understanding of their battery's actual condition.

#### 4 Conclusion and future work

In this paper are presented the design, implementation, and practical validation of a flexible external condition monitoring system for lithium-

ion batteries, specifically targeting light electric vehicles such as e-bikes and e-scooters. By serving as an independent diagnostic interface between the standard power supply and the battery pack, the proposed module effectively addresses the lack of operational transparency in conventional charging setups. The implemented SOH estimation algorithm, based on partial charging extrapolation and discrete energy integration, demonstrated high reliability. It successfully distinguished between healthy battery packs and those with significant capacity fade, without requiring the user to perform time-consuming full discharge cycles.

While the current hardware prototype with a large graphical interface validates the concept, future development will focus on optimizing the device for broader practical deployment. Proposed improvements for future iterations include:

**Cloud-Based Analytics.** Leveraging IoT capabilities for remote data collection and implementing data-driven predictive models to estimate the Remaining Useful Life (RUL) with even greater precision.

**Mobile Application Integration.** Exploiting the native Bluetooth Low Energy (BLE) and Wi-Fi capabilities of the ESP32 microcontroller to transmit data to a dedicated smartphone application (iOS/Android). This app would serve as the primary user interface, offering detailed diagnostic insights, long-term charging history, and degradation trends.

The proposed external monitoring concept transforms a standard charging routine into a reliable diagnostic process, empowering users to maximize the lifespan, safety, and performance of their micromobility energy storage systems.

Future development will include further discussion of specific calibration requirements and device durability under various environmental conditions to streamline integration with commercial charging systems. Additionally, to validate the general applicability and evaluate measurement uncertainties, subsequent research will involve sensitivity analysis, testing on a broader dataset of diverse battery chemistries, and a direct comparative assessment with integrated BMS solutions.

## Acknowledgements

This work was supported by KEGA through the Teaching and development of methodology for the use of microcontrollers in automation using practical examples and laboratory exercises for engineering students under Grant 024STU-4/2024.

## Conflicts of interest

The authors declare that they have no known competing financial interests or personal relationships that could have influenced the work reported in this paper.

## References

- [1] DYCZKOWSKA, J. A., CHAMIER-GLISZCZYNSKI, N., MURAWSKI, J. Assessment of micromobility infrastructure from the perspective of electromobility development. *Applied Sciences* [online]. 2025, **15**(22), 12276. eISSN 2076-3417. Available from: <https://doi.org/10.3390/app152212276>
- [2] MOHAMMADI, F. Lithium-ion battery state-of-charge estimation based on an improved coulomb-counting algorithm and uncertainty evaluation. *Journal of Energy Storage* [online]. 2022, **48**, 104061. ISSN 2352-152X, eISSN 2352-1538. Available from: <https://doi.org/10.1016/j.est.2022.104061>
- [3] PHOGAT, P., DEY, S., WAN, M. Powering the sustainable future: a review of emerging battery technologies and their environmental impact. *RSC Sustainability* [online]. 2025, **3**(8), p. 3266-3306. ISSN 2753-8125. Available from: <https://doi.org/10.1039/D5SU00127G>
- [4] TRAN, M.-K., FOWLER, M. A review of cloud-based battery management systems for lithium-ion batteries in electric vehicles. *IEEE Access* [online]. 2022, **10**, p. 99263-99277. eISSN 2169-3536. Available from: <https://doi.org/10.1109/ACCESS.2024.3446880>
- [5] ARABSALMANABADI, B., TASHAKOR, N., JAVADI, A., AL-HADDAD, K. Charging techniques in lithium-ion battery charger: review and new solution. In: 44th Annual Conference of the IEEE Industrial Electronics Society IECON 2018: proceedings. IEEE. 2018. eISSN 2577-1647, eISBN 978-1-5090-6684-1, p. 5731-5738. Available from: <https://doi.org/10.1109/IECON.2018.8591173>
- [6] OTHMAN, A., HRAD, J., HAJEK, J., MAGA, D. Control strategies of hybrid energy harvesting - a survey. *Sustainability* [online]. 2022, **14**(24), 16670. eISSN 2071-1050. Available from: <https://doi.org/10.3390/su142416670>
- [7] EDGE, J. S., O'KANE, S., PROSSER, R., KIRKALDY, N. D., PATEL, H. C., HALES, A., GHOSH, A., AI, W., CHEN, J., YANG, J., LI, S., PANG, M.-CH., DIAZ, L. B., TOMASZEWSKA, A., MARZOOK, M. V., RADHAKRISHNAN, K. N., WANG, H., PATEL, Y., WUBD, B., OFFER, G. J. Lithium ion battery degradation: what you need to know. *Physical Chemistry Chemical Physics* [online]. 2021, **23**(14), p. 8200-8221. Available from: <https://doi.org/10.1039/D1CP00359C>
- [8] DUAN, J., TANG, X., DAI, H., YANG, Y., WU, W., WEI, X., SUN, Z. Building safe lithium-ion batteries for electric vehicles: a review. *Electrochemical Energy Reviews* [online]. 2020, **3**, p. 1-42. ISSN 2520-8489, eISSN 2520-8136. Available from: <https://doi.org/10.1007/s41918-019-00060-4>
- [9] GAO, W., THOO, A. C., SARKER, M., LEE, N., DENG, X., YANG, Y. Secondary use of retired lithium-ion traction batteries: a review of health assessment, interface technology, and supply chain management. *Batteries* [online]. 2026, **12**(1), 1. eISSN 2313-0105. Available from: <https://doi.org/10.3390/batteries12010001>
- [10] MOVASSAGH, K., RAIHAN, A., BALASINGAM, B., PATTIPATI, K. A critical look at coulomb counting approach for state of charge estimation in batteries. *Energies* [online]. 2021, **14**, 4074. eISSN 1996-1073. Available from: <https://doi.org/10.3390/en14144074>
- [11] PISANI ORTA, M. A., GARCIA ELVIRA, D., VALDERRAMA BLAVI, H. Review of state-of-charge estimation methods for electric vehicle applications. *World Electric Vehicle Journal* [online]. 2025, **16**, 87. eISSN 2032-6653. Available from: <https://doi.org/10.3390/wevj16020087>
- [12] BERICIBAR, M., GANDIAGA, I., VILLARREAL, I., OMAR, N., VAN MIERLO, J., VAN DEN BOSSCHE, P. Critical review of state of health estimation methods of Li-ion batteries for real applications. *Renewable*

- and Sustainable Energy Reviews* [online]. 2016, **56**, p. 572-587. eISSN 1364-0321. Available from: <https://doi.org/10.1016/j.rser.2015.11.042>
- [13] AL-HAJ HUSSEIN, A., BATARSEH, I. A review of charging algorithms for nickel and lithium battery chargers. *IEEE Transactions on Vehicular Technology* [online]. 2011, **60**(3), p. 830-838. ISSN 0018-9545, eISSN 1939-9359. Available from: <https://doi.org/10.1109/TVT.2011.2106527>
- [14] MUN, T., NOH, C., LEE, S.-E. Comparative analysis of DCIR and SOH in field-deployed ESS considering thermal non-uniformity using linear regression. *Energies* [online]. 2025, **18**(21), 5640. eISSN 1996-1073. Available from: <https://doi.org/10.3390/en18215640>
- [15] CHENG, K. W. E., DIVAKAR, B. P., WU, H., DING, K., HO, H. F. Battery-management system (BMS) and SOC development for electrical vehicles. *IEEE Transactions on Vehicular Technology* [online]. 2011, **60**(1), p. 76-88. ISSN 0018-9545, eISSN 1939-9359. Available from: <https://doi.org/10.1109/TVT.2010.2089647>
- [16] TIAN, H., QIN, P., LI, K., ZHAO, Z. A review of the state of health for lithium-ion batteries: research status and suggestions. *Journal of Cleaner Production* [online]. 2020, **261**, 120813. ISSN 0959-6526, eISSN 1879-1786. Available from: <https://doi.org/10.1016/j.jclepro.2020.120813>
- [17] D100v2 AC/DC dual balance charger/discharger/power supply - SkyRC Technology Co., Ltd. [online]. 2022. Available from: [https://www.skyrc.com/D100\\_v2\\_Charger](https://www.skyrc.com/D100_v2_Charger)
- [18] PATTIPATI, B., BALASINGAM, B., AVVARI, G., PATTIPATI, K., BAR-SHALOM, Y. Open circuit voltage characterization of lithium-ion batteries. *Journal of Power Sources* [online]. 2014, **269**, p. 317-333. ISSN 0378-7753, eISSN 1873-2755. Available from: <https://doi.org/10.1016/j.jpowsour.2014.06.152>
- [19] LAVIGNE, L., SABATIER, J., MBALA, F., GUILLEMARD, F., NOURY, A. Lithium-ion open circuit voltage (OCV) curve modelling and its ageing adjustment. *Journal of Power Sources* [online]. 2016, **324**, p. 694-703. ISSN 0378-7753, eISSN 1873-2755. Available from: <https://doi.org/10.1016/j.jpowsour.2016.05.121>